

MIT Open Access Articles

Persistent exciton-type many-body interactions in GaAs quantum wells measured using two-dimensional optical spectroscopy

The MIT Faculty has made this article openly available. **Please share** how this access benefits you. Your story matters.

Citation: Turner, Daniel et al. "Persistent Exciton-type Many-body Interactions in GaAs Quantum Wells Measured Using Two-dimensional Optical Spectroscopy." Physical Review B 85.20 (2012). ©2012 American Physical Society

As Published: <http://dx.doi.org/10.1103/PhysRevB.85.201303>

Publisher: American Physical Society

Persistent URL: <http://hdl.handle.net/1721.1/71685>

Version: Final published version: final published article, as it appeared in a journal, conference proceedings, or other formally published context

Terms of Use: Article is made available in accordance with the publisher's policy and may be subject to US copyright law. Please refer to the publisher's site for terms of use.



Persistent exciton-type many-body interactions in GaAs quantum wells measured using two-dimensional optical spectroscopy

Daniel B. Turner,^{1,*} Patrick Wen,¹ Dylan H. Arias,¹ Keith A. Nelson,^{1,†} Hebin Li,² Galan Moody,² Mark E. Siemens,^{2,‡} and Steven T. Cundiff²

¹*Department of Chemistry, Massachusetts Institute of Technology, Cambridge, Massachusetts 02139, USA*

²*JILA, University of Colorado and National Institute of Standards and Technology, Boulder, Colorado 80309-0440, USA*

(Received 20 April 2011; revised manuscript received 9 February 2012; published 15 May 2012)

Studies have shown that many-body interactions among semiconductor excitons can produce distinct features in two-dimensional optical spectra. However, to the best of our knowledge, the dynamics of many-body interactions have not been measured in two-dimensional (2D) spectroscopy studies. Here we measure 2D spectra of GaAs quantum wells at many different “waiting” times and study the time dependence of the spectral features. Characteristic signatures of exciton polarization correlations manifest in the diagonal peaks decay at the exciton dephasing rate, consistent with theoretical predictions. Other many-body interactions manifest in off-diagonal features decay much more slowly. These persistent off-diagonal features must be due to many-body interactions involving exciton populations, and their persistence cannot be predicted by theoretical descriptions restricted to the coherent limit.

DOI: [10.1103/PhysRevB.85.201303](https://doi.org/10.1103/PhysRevB.85.201303)

PACS number(s): 78.67.De, 42.50.Md, 78.47.jh, 78.47.nj

In many scientific disciplines, groups of objects can interact to produce startling emergent phenomena, that is, “more is different.”¹ In condensed-matter physics, many-body interactions often occur due to the attractions and repulsions among charged particles. These collective effects are difficult to calculate from first principles, making experimental measurements essential to guide our understanding and to motivate and direct theoretical efforts.^{2–6} Semiconductors and their nanostructures offer extraordinary prospects for incisive experimental study of many-body effects because of the following properties: The optically generated excitons are delocalized and weakly bound, enabling Coulomb interactions among their charged electron and hole constituents; the nanostructure dimensionality and dimensions can be designed to confine the excitons so that they must interact; the exciton density can be easily controlled by incident light intensities; and exciton coherences as well as populations can be manipulated by coherent light sources, providing additional avenues for control over many-body interactions and exquisite sensitivity to them in the signals of coherent nonlinear spectroscopy measurements.

GaAs quantum wells were studied extensively^{2–33} throughout the 1980s and 1990s, primarily through four-wave mixing measurements, resulting in new insights about phenomena such as quantum beats, exciton dephasing times and mechanisms, disorder, and many-body interactions. The application of another four-wave mixing technique known as two-dimensional (2D) Fourier-transform optical spectroscopy heralded a new era of investigation.^{34–45} To date, these nonlinear spectroscopy experiments have been understood using theoretical treatments at varying levels of sophistication. Our results show that one of the approximations commonly used in the first-principles treatments is not generally valid.

Two-dimensional spectroscopy is similar to frequency-resolved pump-probe (transient-absorption) spectroscopy;⁴⁶ they are different projections of the same nonlinear signal field produced by three excitation fields, typically femtosecond laser pulses. In pump-probe spectroscopy, the pump beam

electric field interacts twice with the sample to generate a population of electronic excited states. A probe pulse arrives after a variable delay τ_2 to generate a signal that is detected as a change in the transmission of the probe. The measurement thus produces the signal as a function of emission frequency for each time delay, $S(\tau_2, \omega_{\text{emit}})$. This allows extraction of excited-state population lifetimes by tracking the decay of spectral features, but very little information is gained about the excitation process.

In 2D spectroscopy, we introduce a variable time delay between the two pump pulses, τ_1 , which allows us to record and correlate the spectrum of states excited and emitted, $S(\omega_{\text{excite}}, \tau_2, \omega_{\text{emit}})$. The excitation and emission dimensions are produced by Fourier transformation of coherent optical polarizations during the respective time periods. The delay time τ_2 (the “waiting” time) is varied parametrically, and, similar to pump-probe measurements, the changes in spectral features as a function of τ_2 are typically related to incoherent excited-state dynamics. An important feature of 2D spectroscopy is that the phase and amplitude of the emitted signal are sensitive to the phase and amplitude of the coherent excitations produced in the sample by the excitation fields. This *coherence* requirement means that spectral features are sensitive to exciton phases. As shown through phenomenological models,^{33,35,45} many-body interactions can influence the amplitudes and phases of exciton coherences in a variety of ways, and these changes modify the frequency-dependent emission signals that originate with excitation at any of the exciton frequencies. Therefore all of the peaks in a 2D spectrum are sensitive to the presence and the detailed nature of many-body interactions. Previous studies focused on unexpected features produced by many-body interactions in the 2D spectra at $\tau_2 = 0$. Here we vary τ_2 and measure changes to the unexpected features.

Two-dimensional spectral features and the many-body interactions that produce them have been treated through explicit first-principles theoretical calculations of the Coulomb correlations among electrons and holes, performed in the site basis^{4,47,48} or momentum basis.^{6,49,50} The results yielded

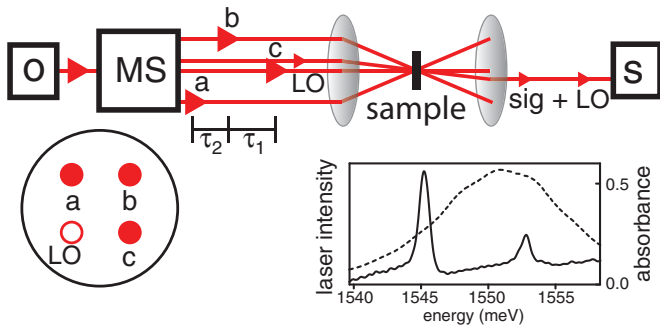


FIG. 1. (Color online) Experimental setup for 2D spectroscopy of GaAs quantum wells. A Ti:sapphire oscillator (O) creates femtosecond pulses in a single beam. The multidimensional spectrometer (MS) transforms this beam into four beams arranged on the corners of a square (inset) and sets the pulse delay times. The beams are then focused to the sample. In the nonrephasing scan (shown), field E_c interacts first, followed first by field E_b after time delay τ_1 and then field E_a after time delay τ_2 . The fields generate a phase-matched signal in the $\mathbf{k}_{\text{sig}} = \mathbf{k}_a - \mathbf{k}_b + \mathbf{k}_c$ direction. In a rephasing or photon echo scan (not shown), the time ordering of fields E_c and E_b is exchanged. In both cases, the resulting signal is overlapped with a weak reference field called a local oscillator (LO) and is heterodyne detected by the spectrometer (S). The 2D spectra displayed in this work are the sum of the rephasing and nonrephasing signals. The absorbance of the sample (solid line) and the spectrum of the laser pulse (dashed line) are also shown.

mean-field polarization-polarization scattering terms that influence the phases of diagonal peaks and, going beyond the Hartree-Fock approximation, four-particle (meaning two-exciton) correlations that give rise to otherwise unexpected off-diagonal spectral features.³⁶ Although the theoretical predictions are in reasonable agreement with experiments,^{35,36,38,41–43,45} to the best of our knowledge, neither theoretical nor prior experimental studies have addressed the time-dependent changes to any of the spectral features during τ_2 . Moreover, all of the microscopic theoretical approaches assumed the *coherent limit* in which the exciton polarization dephasing rate is linked to the exciton population decay rate. In other words, in this limit, effects due to exciton populations cannot be separated from effects due to exciton coherences. 2D spectroscopy measurements conducted at waiting times long enough that exciton polarizations have decayed should allow separation of the two kinds of interactions.

We performed 2D spectroscopy measurements using two experimental apparatuses—the COLBERT spectrometer⁵¹ and the JILA-MONSTR⁵²—that produced the four coherent fields in the beam geometry illustrated in Fig. 1. Briefly, each instrument used a Ti:sapphire oscillator to produce pulses of about 100 fs duration with pulse energies of a few nJ. The spectral bandwidth covered both the heavy-hole exciton (H) and light-hole exciton (L) resonances at 1545 and 1553 meV, respectively. The H exciton linewidth indicates a dephasing time of about 10 ps. Experiments at MIT (JILA) were conducted with an excitation density of about 3×10^{10} excitons/cm²/well (4.5×10^9 excitons/cm²/well) in a sample that consisted of ten (four) layers of 10 nm thick GaAs, separated by 10 nm thick Al_{0.3}Ga_{0.7}As barriers. The exciton population lifetimes are on the order of a hundred picoseconds

at these densities. In all measurements, the sample was cooled to 10 K and the laser fields were co-circularly polarized. The spectra were phased using the established procedure for each apparatus.^{51,53} We present data taken with the JILA-MONSTR; the qualitative features were reproduced in the data taken with the COLBERT spectrometer on a different sample. The difference between the data sets was the decay time of the features. In the MIT measurements, the decay time of the symmetry factor (see below) was faster than 3 ps; this was due to the delay-dependent amplitude modulation of the COLBERT spectrometer.⁵¹ The similarity of the observations confirms that they are not due to experimental issues, such as phase drift in the spectrometer, and that they are not unique to one sample.

Rephasing (nonrephasing) spectra were collected when field E_b (E_c) interacted first, followed after time period τ_1 by field E_c (E_b), for each value of τ_2 . The rephasing and nonrephasing spectra were measured independently and then summed to create the 2D spectra displayed in Fig. 2. Rephasing or nonrephasing spectra alone are not sufficient to extract true line shapes because the individual spectra have wings due to “phase twist”; taking the sum of the two spectra removes the mixing between the absorptive and dispersive characters.^{54,55} An absorptive line shape is typically Lorentzian in character, while a dispersive line shape is typically similar to the derivative of a Lorentzian. In a 2D spectrum of a simple system, peaks will have absorptive line shapes, cross peaks will only appear between coupled transitions, excited-state-absorption pathways will lead to negative-amplitude peaks, and additional features are not observed. The shape of a peak indicates the relative contributions of homogeneous and inhomogeneous dephasing mechanisms. We extracted a homogeneous dephasing time of 5.0 ± 0.1 ps from the amplitude of the rephasing signal of the H diagonal peak using a fit procedure described previously.⁵⁶

We display only the real parts of the complex-valued spectra in Fig. 2 for selected values of τ_2 . With co-circularly polarized pulses, cross peaks are not expected because the H and L excitons have electrons which reside in different conduction bands⁵ and therefore the transitions that generate the two excitons are not coupled through a common spectroscopic ground state. However, as shown in Fig. 2, cross peaks labeled X'' and X' do appear. Strong vertical features, also previously observed,³⁴ are due to scattering between excitons and free carriers. The cross peaks and vertical features have been reproduced in microscopic theories by including four-particle interaction terms into the equations of motion.³⁶ Below we show that since these spectral features persist at long τ_2 times, this assignment was incomplete.

The strongest peak in Fig. 2—the H diagonal peak highlighted in the red square—has a dispersive line shape at small values of τ_2 , in agreement with previous rephasing measurements.^{35,38,42} As τ_2 increases, the positive part becomes stronger than the negative part and shifts toward the diagonal line. At very long τ_2 times, the peak has an absorptive line shape and is centered on the diagonal line. During this transition from dispersive to absorptive, the nodal line tilts from being parallel to the diagonal line to being completely vertical, indicating a loss of correlation⁵⁴ among multiple excitons.

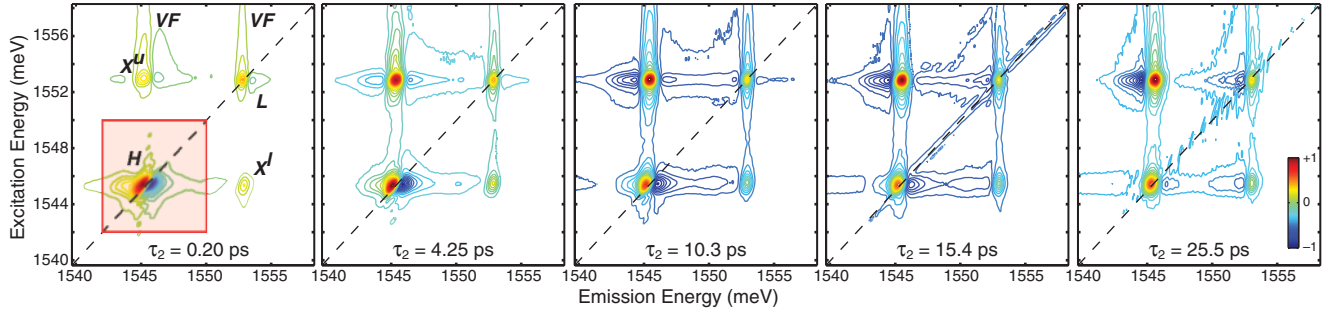


FIG. 2. (Color online) The real part of the 2D spectra under co-circular polarization measured at the indicated waiting times (τ_2). The dashed line indicates the diagonal, $E_{\text{excite}} = E_{\text{emit}}$, and the red box highlights the H diagonal peak. Cross peaks between the H and L features are not expected in this polarization configuration in the absence of many-body interactions because the two excitons do not share a common conduction band. Coulomb correlations couple the two states, leading to cross peaks labeled X'' and X' . Vertical features (VF) are due to exciton-free-carrier scattering.

To understand better the line-shape change, we project the H diagonal peak onto the emission axis and plot the projections in Fig. 3(a) for selected values of τ_2 . The line shape changes systematically from an antisymmetric shape to a symmetric shape. Since the peak symmetry reflects how dispersive the line shape is, we define a *symmetry factor* (η) given by

$$\eta(\tau_2) = \frac{\int p(\tau_2, \omega_{\text{emit}}) d\omega_{\text{emit}}}{\int |p(\tau_2, \omega_{\text{emit}})| d\omega_{\text{emit}}}, \quad (1)$$

where $p(\tau_2, \omega_{\text{emit}})$ is the projection of the signal inside the red square as a function of emission energy at a particular waiting time. Using this equation, a purely dispersive line shape corresponds to $\eta = 0$ and a purely absorptive line shape with a positive (negative) amplitude corresponds to $\eta = 1$ ($\eta = -1$). The symmetry factors retrieved from the 2D spectra at 11 τ_2 values are shown in Fig. 3(b). Initially, $\eta = 0$; it then increases and saturates at $\eta = 1$ by about 20 ps. As mentioned above, rephasing or nonrephasing spectra alone are not sufficient to extract the data presented in Fig. 3.

The normalized amplitudes of the H and X' peaks during τ_2 are shown in Fig. 3(b). The data were created by integrating over a square that covered each peak in the amplitude (not real part) of the 2D spectra to account for any changes to the shape of the peaks. Due to the projection-slice theorem, it should be possible, at least in principle, to measure the data presented in Fig. 3 using a narrow-band, frequency-resolved pump-probe measurement, but it would be difficult to draw conclusions about many-body interactions since the cross peaks and vertical features would not be visible.

The measurements reveal a key insight about many-body interactions in GaAs quantum wells. The dispersive line shape of the H diagonal peak is characteristic of many-body interactions, whereas the absorptive line shape is more characteristic of the case without many-body interactions, for example, including only simple Pauli-blocking terms³⁶ which account for the reduction of allowed transitions for fermions due to the Pauli exclusion principle. The fact that the cross peaks and vertical features do not disappear at long waiting times means that the many-body terms have not vanished. In principle, incoherent population relaxation from high-energy states (unbound electron-hole pairs and L excitons) to H could be responsible for the continued presence of X'' and the vertical features. However, as shown in Fig. 3(b), the X' peak—which

cannot be due to incoherent relaxation—has only decayed to about half its original amplitude at 35 ps. Thus we conclude

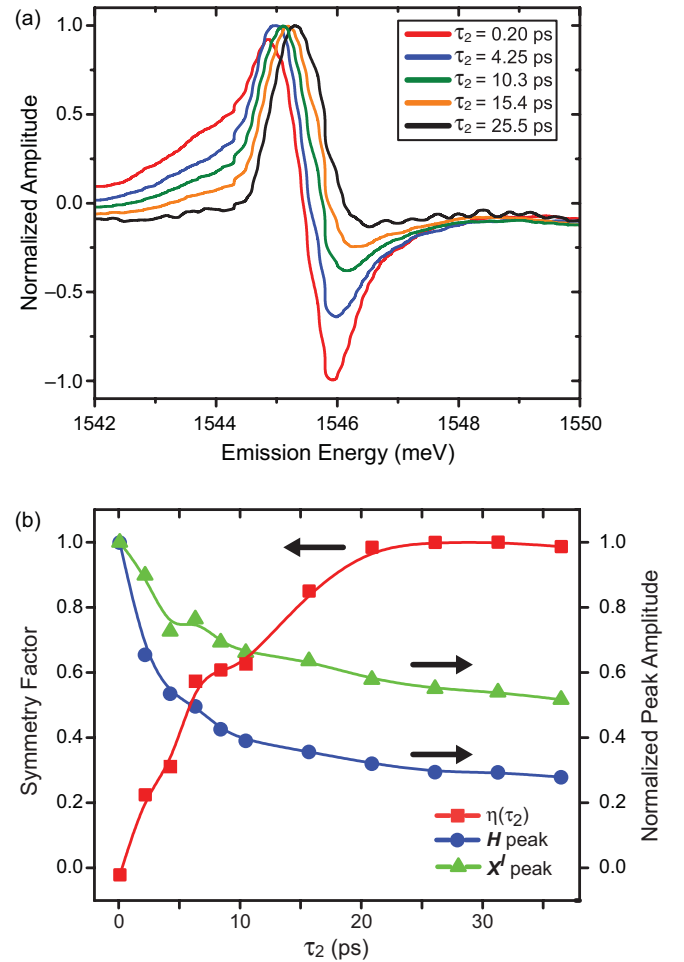


FIG. 3. (Color online) Peak and line-shape dynamics extracted from the 2D spectra. (a) Projections of the H diagonal peak onto the emission axis for the indicated τ_2 values. (b) Extracted symmetry factor and the normalized amplitudes of the H diagonal peak and the X' cross peak at several τ_2 values. Lines are guides to the eye. The decay of the symmetry factor reflects the decay of the polarization-polarization scattering terms. Both H and X' retain nonzero amplitudes at 35 ps.

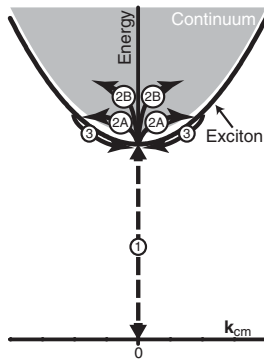


FIG. 4. Schematic showing the energy vs center-of-mass momentum (\mathbf{k}_{cm}) for electron-hole pairs bound into excitons (bold line) and unbound pairs that form a continuum (gray area). Excitation by light (1) produces an excitonic polarization at $\mathbf{k}_{\text{cm}} = 0$ that rapidly scatters to excitonic polarizations and populations at $|\mathbf{k}_{\text{cm}}| > 0$ (2A) and to unbound pairs (2B) in the continuum. The resulting many-body configuration then evolves (3) as the polarizations decay and the populations relax back toward $\mathbf{k}_{\text{cm}} = 0$.

that the evolution of the spectra must reflect evolution of the many-body state. Specifically, we suggest that the dispersive line shape is due to polarization-polarization scattering, and the polarizations decay on picosecond time scales, while many-body interactions involving exciton populations persist, leading to the unanticipated spectral features at long τ_2 times.

In the momentum basis, the polarization scattering effect can be understood in the following manner. First, the light generates an excitonic polarization with $\mathbf{k}_{\text{cm}} = 0$ (arrow 1 in Fig. 4). Due to carrier-carrier scattering and carrier-phonon scattering, this initial excitonic polarization is scattered to excitonic polarizations and populations at larger \mathbf{k}_{cm} (arrows 2A, the arrow represents scattering into both polarization and population states). The excitonic polarization can also scatter into unbound electron-hole states, which form a continuum (arrows 2B), but at the low excitation densities used here this process is less important. These processes happen very rapidly, but the subsequent evolution of the many-body configuration as carriers scatter toward a thermal distribution (arrows 3) is slower. A true thermal equilibrium is not achieved within the time window of our experiments because of radiative recombination of excitons within the light-cone (close to $\mathbf{k}_{\text{cm}} = 0$) (see Fig. 38 in Ref. 49). Careful comparison between experiment and theory have shown that the excitonic line shape

in linear absorption spectra can be used to estimate the many-body configuration.⁵⁰ Thus, at short delay the presence of excitonic polarizations results in a very different line shape than for longer delays where the excitonic polarizations have decayed and only populations remain. Our results use the evolution of the 2D line shape to monitor the dynamics of the many-body states as it evolves from a mixture of polarizations and populations to being purely populations.

In our experiments, the behavior shown in Fig. 3 depends strongly on the sample position. The rise time, which is about 20 ps in the presented case, varies over a wide range under identical conditions except for a change in sample position. In some cases, the rise time is so long that $\eta = 0$ for almost the entire window of nearly 40 ps. This spatial inhomogeneity could be caused by stress due to differences in thermal expansion since the sample is mounted on a sapphire disk. A comparison of the absorption spectra at different spots on the sample showed frequency shifts (but no linewidth changes) for the H and L resonances. A larger frequency shift corresponded to a longer rise time in η . However, an explanation of the detailed mechanism requires further investigation.

We have measured 2D optical spectra of excitons in GaAs quantum wells using co-circularly polarized beams for waiting times out to nearly 40 ps. Our results provide unique insight into the evolution of the optically induced many-body state and show that the effect of polarization-polarization scattering decays on picosecond time scales, but several spectral features that were previously attributed to coherent four-particle interactions persist. We attribute those features to many-body interactions involving exciton populations. This observation means that different theoretical models are needed that do not assume the coherent limit,^{4,36,47} where the signal decay is governed solely by exciton dephasing. Additionally, since, to the best of our knowledge, calculations of many-body states⁵⁰ have not included dynamics, our observations should motivate the development of a dynamical many-body theory for optically excited semiconductors.

D.B.T. was financially supported by NDSEG and NSF. P.W. was supported as part of the DOE BES-EFRC Award No. DE-SC0001088. The work at MIT was supported in part by NSF Grants No. CHE-0616939 and No. CHE-1111557. The work at JILA was supported by the Chemical Sciences, Geosciences, and Energy Biosciences Division, Office of Basic Energy Science, Office of Science, US Department of Energy and the NSF.

*Present address: Department of Chemistry and Centre for Quantum Information and Quantum Control, 80 Saint George Street, University of Toronto, Toronto, Ontario, M5S 3H6 Canada.

†kanelson@mit.edu

‡Present address: Department of Physics and Astronomy, University of Denver, Denver, CO 80208-6900.

¹P. W. Anderson, *Science* **177**, 393 (1972).

²J. Shah, *Ultrafast Spectroscopy of Semiconductors and Semiconductor Nanostructures* (Springer, Berlin, 1999).

³D. S. Chemla and J. Shah, *Nature (London)* **411**, 549 (2001).

⁴T. Meier, P. Thomas, and S. Koch, *Coherent Semiconductor Optics: From Basic Concepts to Nanostructure Applications* (Springer, Berlin, 2007).

⁵S. T. Cundiff, *Opt. Express* **16**, 4639 (2008).

⁶H. Haug and S. W. Koch, *Quantum Theory of the Optical and Electronic Properties of Semiconductors* (World Scientific, New Jersey, 2009).

- ⁷J. Hegarty, M. D. Sturge, A. C. Gossard, and W. Wiegmann, *Appl. Phys. Lett.* **40**, 132 (1982).
- ⁸D. A. B. Miller, D. S. Chemla, D. J. Eilenberger, P. W. Smith, A. C. Gossard, and W. Wiegmann, *Appl. Phys. Lett.* **42**, 925 (1983).
- ⁹L. Schultheis, M. D. Sturge, and J. Hegarty, *Appl. Phys. Lett.* **47**, 995 (1985).
- ¹⁰D. S. Chemla and D. A. B. Miller, *J. Opt. Soc. Am. B* **2**, 1155 (1985).
- ¹¹S. Schmitt-Rink, D. S. Chemla, and D. A. B. Miller, *Phys. Rev. B* **32**, 6601 (1985).
- ¹²L. Schultheis, J. Kuhl, A. Honold, and C. W. Tu, *Phys. Rev. Lett.* **57**, 1797 (1986).
- ¹³L. Schultheis, A. Honold, J. Kuhl, K. Köhler, and C. W. Tu, *Phys. Rev. B* **34**, 9027 (1986).
- ¹⁴M. Lindberg and S. W. Koch, *Phys. Rev. B* **38**, 3342 (1988).
- ¹⁵A. Honold, L. Schultheis, J. Kuhl, and C. W. Tu, *Phys. Rev. B* **40**, 6442 (1989).
- ¹⁶K. Leo, M. Wegener, J. Shah, D. S. Chemla, E. O. Göbel, T. C. Damen, S. Schmitt-Rink, and W. Schafer, *Phys. Rev. Lett.* **65**, 1340 (1990).
- ¹⁷M. Wegener, D. S. Chemla, S. Schmitt-Rink, and W. Schäfer, *Phys. Rev. A* **42**, 5675 (1990).
- ¹⁸M. Koch, J. Feldmann, G. von Plessen, E. Göbel, P. Thomas, and K. Köhler, *Phys. Rev. Lett.* **69**, 3631 (1992).
- ¹⁹J. Feldmann, T. Meier, G. von Plessen, M. Koch, E. O. Göbel, P. Thomas, G. Bacher, C. Hartmann, H. Schweizer, W. Schäfer, and H. Nickel, *Phys. Rev. Lett.* **70**, 3027 (1993).
- ²⁰A. Lohner, K. Rick, P. Leisching, A. Leitenstorfer, T. Elsaesser, T. Kuhn, F. Rossi, and W. Stolz, *Phys. Rev. Lett.* **71**, 77 (1993).
- ²¹V. G. Lyssenko, J. Erland, I. Balslev, K. H. Pantke, B. S. Razbirin, and J. M. Hvam, *Phys. Rev. B* **48**, 5720 (1993).
- ²²V. M. Axt and A. Stahl, *Z. Phys. B* **93**, 195 (1994).
- ²³A. Leitenstorfer, A. Lohner, K. Rick, P. Leisching, T. Elsaesser, T. Kuhn, F. Rossi, W. Stolz, and K. Ploog, *Phys. Rev. B* **49**, 16372 (1994).
- ²⁴M. Koch, R. Hellmann, G. Bastian, J. Feldmann, E. O. Göbel, and P. Dawson, *Phys. Rev. B* **51**, 13887 (1995).
- ²⁵S. T. Cundiff, M. Koch, W. H. Knox, J. Shah, and W. Stolz, *Phys. Rev. Lett.* **77**, 1107 (1996).
- ²⁶X. Chen, W. J. Walecki, O. Buccafusca, D. N. Fittinghoff, and A. L. Smirl, *Phys. Rev. B* **56**, 9738 (1997).
- ²⁷V. M. Axt and S. Mukamel, *Rev. Mod. Phys.* **70**, 145 (1998).
- ²⁸K. B. Ferrio and D. G. Steel, *Phys. Rev. Lett.* **80**, 786 (1998).
- ²⁹G. Manzke, Q. Y. Peng, K. Henneberger, U. Neukirch, K. Hauke, K. Wundke, J. Gutowski, and D. Hommel, *Phys. Rev. Lett.* **80**, 4943 (1998).
- ³⁰M. Phillips and H. Wang, *Solid State Commun.* **111**, 317 (1999).
- ³¹A. L. Smirl, M. J. Stevens, X. Chen, and O. Buccafusca, *Phys. Rev. B* **60**, 8267 (1999).
- ³²S. R. Bolton, U. Neukirch, L. J. Sham, D. S. Chemla, and V. M. Axt, *Phys. Rev. Lett.* **85**, 2002 (2000).
- ³³J. M. Shacklette and S. T. Cundiff, *Phys. Rev. B* **66**, 045309 (2002).
- ³⁴C. N. Borca, T. Zhang, X. Li, and S. T. Cundiff, *Chem. Phys. Lett.* **416**, 311 (2005).
- ³⁵X. Li, T. Zhang, C. N. Borca, and S. T. Cundiff, *Phys. Rev. Lett.* **96**, 057406 (2006).
- ³⁶T. Zhang, I. Kuznetsova, T. Meier, X. Li, R. P. Mirin, P. Thomas, and S. T. Cundiff, *Proc. Natl. Acad. Sci. USA* **104**, 14227 (2007).
- ³⁷L. Yang, T. Zhang, A. D. Bristow, S. T. Cundiff, and S. Mukamel, *J. Chem. Phys.* **129**, 234711 (2008).
- ³⁸A. D. Bristow, D. Karauskaj, X. Dai, R. P. Mirin, and S. T. Cundiff, *Phys. Rev. B* **79**, 161305(R) (2009).
- ³⁹X. Li, T. Zhang, S. Mukamel, R. P. Mirin, and S. T. Cundiff, *Solid State Commun.* **149**, 361 (2009).
- ⁴⁰K. W. Stone, D. B. Turner, K. Gundogdu, S. T. Cundiff, and K. A. Nelson, *Acc. Chem. Res.* **42**, 1452 (2009).
- ⁴¹K. W. Stone, K. Gundogdu, D. B. Turner, X. Li, S. T. Cundiff, and K. A. Nelson, *Science* **324**, 1169 (2009).
- ⁴²D. B. Turner, K. W. Stone, K. Gundogdu, and K. A. Nelson, *J. Chem. Phys.* **131**, 144510 (2009).
- ⁴³D. B. Turner and K. A. Nelson, *Nature (London)* **466**, 1089 (2010).
- ⁴⁴J. A. Davis, C. R. Hall, L. V. Dao, K. A. Nugent, H. M. Quiney, H. H. Tan, and C. Jagadish, *J. Chem. Phys.* **135**, 044510 (2011).
- ⁴⁵D. B. Turner, P. Wen, D. H. Arias, and K. A. Nelson, *Phys. Rev. B* **84**, 165321 (2011).
- ⁴⁶S. Mukamel, *Principles of Nonlinear Optical Spectroscopy* (Oxford University Press, New York, 1995).
- ⁴⁷L. Yang, I. V. Schweigert, S. T. Cundiff, and S. Mukamel, *Phys. Rev. B* **75**, 125302 (2007).
- ⁴⁸L. Yang and S. Mukamel, *Phys. Rev. B* **77**, 075335 (2008).
- ⁴⁹M. Kira and S. W. Koch, *Prog. Quantum Electron.* **30**, 155 (2006).
- ⁵⁰R. P. Smith, J. K. Wahlstrand, A. C. Funk, R. P. Mirin, S. T. Cundiff, J. T. Steiner, M. Schafer, M. Kira, and S. W. Koch, *Phys. Rev. Lett.* **104**, 247401 (2010).
- ⁵¹D. B. Turner, K. W. Stone, K. Gundogdu, and K. A. Nelson, *Rev. Sci. Instrum.* **82**, 081301 (2011).
- ⁵²A. D. Bristow, D. Karauskaj, X. Dai, T. Zhang, C. Carlsson, K. R. Hagen, R. Jimenez, and S. T. Cundiff, *Rev. Sci. Instrum.* **80**, 073108 (2009).
- ⁵³A. D. Bristow, D. Karauskaj, X. Dai, and S. T. Cundiff, *Opt. Express* **16**, 18017 (2008).
- ⁵⁴N. Demirdöven, M. Khalil, and A. Tokmakoff, *Phys. Rev. Lett.* **89**, 237401 (2002).
- ⁵⁵M. Khalil, N. Demirdöven, and A. Tokmakoff, *Phys. Rev. Lett.* **90**, 047401 (2003).
- ⁵⁶M. E. Siemens, G. Moody, H. Li, A. D. Bristow, and S. T. Cundiff, *Opt. Express* **18**, 17699 (2010).